AGMC-Based Robust Cubature Kalman Filter for SINS/GNSS Integrated Navigation System With Unknown Noise Statistics

KAIQIANG FENG[1], **JIE LI**[2], **DEBIAO ZHANG**[1], **XIAOKAI WEI**[1], AND **JIANPING YIN**[3]

[1]Key Laboratory of Instrumentation Science & Dynamic Measurement, Ministry of Education, North University of China, Taiyuan 030051, China
[2]National Key Laboratory for Electronic Measurement Technology, North University of China, Taiyuan 030051, China
[3]College of Mechatronics Engineering, North University of China, Taiyuan 030051, China

Corresponding author: Jie Li (lijie@nuc.edu.cn)

ABSTRACT A new robust cubature Kalman filter is proposed using adaptive generalized maximum correntropy (AGMC) criterion rather than the conventional MMSE criterion in this paper. In the proposed method, the adaptive generalized maximum correntropy (AGMC) criterion is firstly constructed from an adaptive forgetting correntropy based cost function, which is rather robust with respect to the process uncertainty and non-Gaussian noise. On this basis, a new robust cubature Kalman filter is further derived, where the predicted state vector and received measurements are processed simultaneously based on the regression form derived via the statistical linearization approach. An adaptive forgetting scheme is then proposed in combination with the AGMC-CKF to update the parameters of the AGMC adaptively in real time. Taking advantage of the AGMC, the unknown noise statistics caused by the process uncertainty and non-Gaussian noise can be effectively suppressed. Simulations and car-mounted experiments demonstrate that the proposed filter is superior in terms of estimation accuracy and robustness as compared with the related state-of-art methods.

INDEX TERMS SINS/GNSS integrated navigation system, robust estimation, cubature Kalman filter, dynamic state estimation.

I. INTRODUCTION

Because of the complementary properties of the strap-down inertial navigation system (SINS) and global navigation satellite system (GNSS), the integration of SINS and GNSS has become one of the most popular approaches to the position and attitude determination of a moving vehicle [1]–[3]. The high-dimensional nonlinear SINS/GNSS integrated navigation system widely applies the cubature Kalman filter (CKF) featuring satisfactory performance and ease of implementation [4], [5]. The CKF is developed based on the minimum mean square error (MMSE) criterion and only suitable for the Gaussian system with exact prior knowledge of process noise and measurement noise [6]. However, in the practical applications, due to the vehicle's severe maneuver and

abnormal measurement of GNSS, the process noise of the SINS/GNSS integrated navigation system is hard to obtain and the measurement noise may not follow the Gaussian distribution, thus causing a negative impact on the system performance [7]–[9]. Therefore, this work is aimed to develop an effective CKF to increase the estimation accuracy and robustness against both of the uncertain process noise and non-Gaussian measurement noise.

Recently, the adaptive Kalman filter (AKF) theory has attracted wide attention and been extensively employed to deal with the uncertain dynamic system. Existing methods based on the AKF theory can be categorized into three groups, i.e., multi-model adaptive estimation, adaptive stochastic modeling, and covariance scaling. The multiple model AKF (MMAKF), a multi-model adaptive estimation method, captures the uncertain process noise by running a bank of Kalman filters with different stochastic models parally [10].

The associate editor coordinating the review of this manuscript and approving it for publication was Farid Boussaid.

However, it operates under the assumption that one of the models in the model bank is correct, limiting its application to systems with known dynamics [11]. The innovation-based AKF (IAKF) is an adaptive stochastic modeling method, which estimates the appropriate covariance matrix of process noise by forcing the innovation sequence of the Kalman filter to be white Gaussian noise sequence with zero mean [12]. However, the convergence to the right process noise covariance matrix cannot be guaranteed and rather large windows of data are required to achieve a reliable estimation of process noise covariance matrix, making it only applicable to slowly changing systems [13]. The strong tracking filter (STF) is a covariance scaling method targeting the uncertain dynamic system, which introduces the time-variant fading factor to the state prediction covariance matrix [14], [15]. However, the difficulty in determining the true value of the fading factor in practical application results in a limited estimation accuracy [16].

Existing methods for the robustness against non-Gaussian measurement noise includes the particle filter (PF) [17]–[19], robust student's t nonlinear filter (RSTNF) [20]–[22] and Maximum Correntropy Criterion Kalman filter (MCC-KF) [23]–[25]. To solve the non-Gaussian state estimation problem, the PF utilizes a set of random particles to approximate the posterior probability distribution of the system state. However, in the high-dimensional SINS/GNSS integrated navigation system, it is subject to the substantial computational complexity, which increases exponentially with the dimension of the state [26]. The RSTNF copes with the non-Gaussian measurement noise by modeling the heavy-tailed non-Gaussian noise as student's t distribution, which has heavier tails than the Gaussian distribution. However, the growth of the degree of freedom (DOF) may reduce the estimation accuracy of the RSTNF [22]. The MCC-KF deals with the non-Gaussian noise by maximizing the Gaussian correntropy function of one-step prediction error and residual. Its performance depends largely on the selection of Gaussian-kernel width. However, the determination methods for the proper Gaussian-kernel width is lack of a theoretical basis in actual SINS/GNSS integrated navigation applications, which adversely impacts the performance of MCC-KF [27].

To overcome the aforementioned challenges, a new robust filtering algorithm is proposed here for a class of uncertain and non-Gaussian SINS/GNSS integrated systems. This paper provides an integrated and comprehensive method to improve the conventional CKF-based integration approach. Its contributions are summarized below:

(1) The statistical linearization method is presented to construct the general batch-mode linear regression model. On this basis, the non-Gaussian measurement noise existed in both of the linear and nonlinear dynamic systems can be suppressed by using the maximum correntropy approach.

(2) The adaptive generalized maximum correntropy criterion (AGMC) based on the batch-mode regression model is

proposed to process the predicted state vector and the measurement simultaneously, yielding a new form of robust filter.

(3) An adaptive forgetting scheme in combination with the AGMC-CKF is further developed to update AGMC parameters adaptively in real time, displaying a good performance in suppressing process uncertainty.

(4) A hypothesis test method based on Mahalanobis distance is presented to detect observation and innovation outliers, as well as avoid numerical singular in the calculation of the measured noise covariance matrix.

The rest of paper is organized as follows. Section II presents the problem formulation, followed by the introduction of the proposed AGMC-CKF in Section III and the discussion of simulation and experimental results in Section IV. Finally, conclusions are drawn in Section V.

II. PROBLEM FORMULATION
A. NONLINEAR SINS/GNSS INTEGRATED NAVIGATION SYSTEM MODEL

The nonlinear discrete-time dynamic system with additive noise is expressed as follows:

$$\begin{cases} \mathbf{x}_k = f(\mathbf{x}_{k-1}) + \mathbf{w}_{k-1} \\ \mathbf{z}_k = h(\mathbf{x}_k) + \mathbf{v}_k \end{cases} \tag{1}$$

where $\mathbf{x}_k \in \mathbb{R}^{n \times 1}$ and $\mathbf{z}_k \in \mathbb{R}^{m \times 1}$ are respectively the n-dimensional system state vector and m-dimensional measurement vector at time step k. $f(\cdot)$ and $h(\cdot)$ are respectively the nonlinear dynamic system model and measurement model. $\mathbf{w}_{k-1}$ and $\mathbf{v}_k$ are respectively the system process and measurement noise, which are assumed to be Gaussian white noise sequences with zero means and variance matrices $\mathbf{Q}_{k-1}$ and $\mathbf{R}_k$, respectively.

The SINS body frame (Front-Up-Right) is denoted by b; n indicates the local level navigation frame (North-Up-East); e refers to the earth frame; i represents the inertial frame. In this paper, we define the 21-dimension state vector for the low-cost SINS/GNSS integrated navigation system as follows:

$$\mathbf{x} = \begin{bmatrix} \varphi^n & \delta\mathbf{v}^n & \delta\mathbf{p}^n & \mathbf{b}_g & \mathbf{b}_f & \delta\mathbf{b}_g & \delta\mathbf{b}_f \end{bmatrix}^T$$

where $\varphi^n = \begin{bmatrix} \varphi_N & \varphi_u & \varphi_E \end{bmatrix}$ is the misalignment angle between the calculated navigation frame and true navigation frame with φ_N, φ_u and φ_E being respectively the north, up and east misalignment angle error. $\delta\mathbf{v}^n = [\delta V_N \; \delta V_u \; \delta V_E]$ denotes the velocity error component in north, up, and east direction. $\delta\mathbf{p}^n = [\delta\lambda \; \delta L \; \delta h]$ is the position error with $\delta\lambda$, δL and δh being respectively the longitude error, latitude error and height error. $\mathbf{b}_g$ and $\delta\mathbf{b}_g$ denote the static and dynamic bias of the tri-axis gyroscope, respectively. $\mathbf{b}_f$ and $\delta\mathbf{b}_f$ are respectively the static and dynamic biases of the tri-axis accelerometer. According to [5], the nonlinear system error

equation of SINS can be formulated as follows:

$$
\begin{cases}
\dot{\varphi}^n = \mathbf{C}_w^{-1} \left[\left(\mathbf{I} - \mathbf{C}_n^p\right) w_{in}^n + \delta w_{in}^n - \mathbf{C}_b^p \delta w_{ib}^b \right] \\
\delta \dot{\mathbf{v}}^n = \left(\mathbf{I} - \mathbf{C}_p^n\right) \mathbf{C}_b^p f_{ib}^b + \mathbf{C}_b^p \delta f_{ib}^b + \delta \mathbf{v}^n \times \left(2 w_{ie}^n + w_{en}^n\right) \\
\quad + \mathbf{v}^n \times \left(2 \delta w_{ie}^n + \delta w_{en}^n\right) \\
\delta \dot{\lambda} = \dfrac{\delta V_E}{R_N + h} \sec L + \delta L \dfrac{V_E \sec L}{R_N + h} \tan L \\
\delta \dot{L} = \dfrac{\delta V_N}{R_N + h} \\
\delta \dot{h} = \delta V_U \\
\dot{b}_g = 0 \\
\dot{b}_f = 0 \\
\delta \dot{b}_g = -\dfrac{1}{\tau_g} \delta b_g + \eta_g \\
\delta \dot{b}_f = -\dfrac{1}{\tau_f} \delta b_f + \eta_f
\end{cases}
\tag{2}
$$

where $\mathbf{C}_w^{-1}$ denotes the transformation matrix from angle rate to Euler angle, $\mathbf{C}_n^p$ and $\mathbf{C}_b^p$ denote the attitude rotation matrix from n-frame (ideal navigation frame) to p-frame (actual navigation frame) and b-frame (body frame) to p-frame, respectively; ω_{ba}^c denotes the rotation velocity of a-frame with respected to b-frame expressed in c-frame, and $\delta \omega_{ba}^c$ denotes the corresponding error; $\mathbf{R}_N$ is the normal radius; τ_g and τ_f are respectively the correlation time of 1st-order Markovian process for gyroscope and accelerometer; η_g and η_f denote the zero-mean Gaussian white noise process.

In this paper, the loosely coupled method is adopted for the integration of SINS and GNSS. In the state space model of SINS/GNSS integrated navigation system, the SINS error equation is utilized as the system process model and the measurement vector is determined from the position error between SINS and GNSS. Thus, the state transition function $f(\cdot)$ can be obtained from (2). The measurement vector can be expressed as

$$
\mathbf{z}_k = \begin{bmatrix} \mathbf{V}_{GNSS} - \mathbf{V}_{SINS} \\ L_{GNSS} - L_{SINS} \\ h_{GNSS} - h_{SINS} \\ \lambda_{GNSS} - \lambda_{SINS} \end{bmatrix},
$$

with the subscripts (GNSS and SINS) being the velocity and geographical position obtained from GNSS and SINS, respectively. The observation matrix can be formulated as $h(\mathbf{x}_k) = [\mathbf{0}_{6 \times 3}, \mathbf{I}_{6 \times 6}, \mathbf{0}_{6 \times 12}]$.

B. DYNAMIC STATE ESTIMATION USING CKF

The procedure for the high dimensional nonlinear dynamic system state estimation using CKF can be summarized as follows [28]:

Time Update: Assuming the state estimate $\hat{\mathbf{x}}_{k-1|k-1}$ and variance matrix $\mathbf{P}_{k-1|k-1}$ at time step k-1 is known, the cubature points for $i = 1, \ldots, 2n$ with weight $\omega_i = \frac{1}{2n}$ are calculated as follows:

$$
\mathbf{X}_{i,k-1|k-1} = \hat{\mathbf{x}}_{k-1|k-1} \pm \left(\sqrt{n \mathbf{P}_{k-1|k-1}}\right)_i \tag{3}
$$

Then, the cubature points are propagated through the nonlinear system process model as follows:

$$
\mathbf{X}_{i,k|k-1}^* = f\left(\mathbf{X}_{i,k-1|k-1}\right) \tag{4}
$$

Next, the predicted states and the corresponding covariance matrix are calculated as follows:

$$
\hat{\mathbf{x}}_{k|k-1} = \frac{1}{2n} \sum_{i=1}^{2n} \mathbf{X}_{i,k|k-1}^* \tag{5}
$$

$$
\mathbf{P}_{k|k-1} = \frac{1}{2n} \sum_{i=1}^{2n} \mathbf{X}_{i,k|k-1}^* \mathbf{X}_{i,k|k-1}^{*T} - \hat{\mathbf{x}}_{k|k-1} \hat{\mathbf{x}}_{k|k-1}^T + \mathbf{Q}_{k-1} \tag{6}
$$

Measurement Update: Based on the predicted states $\hat{\mathbf{x}}_{k|k-1}$ and the corresponding covariance matrix $\mathbf{P}_{k|k-1}$, the cubature points for $i = 1, \ldots, 2n$ with weight $\omega_i = \frac{1}{2n}$ are calculated as follows:

$$
\mathbf{X}_{i,k|k-1} = \hat{\mathbf{x}}_{k|k-1} \pm \left(\sqrt{n \mathbf{P}_{k|k-1}}\right)_i \tag{7}
$$

Then, the cubature points are propagated through the nonlinear measurement model as follows:

$$
\mathbf{Z}_{i,k|k-1} = h\left(\mathbf{X}_{i,k|k-1}\right) \tag{8}
$$

Next, the predicted measurement vector $\hat{\mathbf{z}}_{k|k-1}$, covariance matrix $\mathbf{P}_{zz,k|k-1}$, and cross-covariance matrix $\mathbf{P}_{xz,k|k-1}$ are respectively calculated as follows:

$$
\hat{\mathbf{z}}_{k|k-1} = \frac{1}{2n} \sum_{i=1}^{2n} \mathbf{Z}_{i,k|k-1} \tag{9}
$$

$$
\mathbf{P}_{zz,k|k-1} = \frac{1}{2n} \sum_{i=1}^{2n} \mathbf{Z}_{i,k|k-1} \mathbf{Z}_{i,k|k-1} - \hat{\mathbf{z}}_{k|k-1} \hat{\mathbf{z}}_{k|k-1}^T + R_k \tag{10}
$$

$$
\mathbf{P}_{xz,k|k-1} = \frac{1}{2n} \sum_{i=1}^{2n} \mathbf{X}_{i,k|k-1} \mathbf{Z}_{i,k|k-1}^T - \hat{\mathbf{x}}_{k|k-1} \hat{\mathbf{z}}_{k|k-1}^T \tag{11}
$$

Finally, the posterior state $\hat{\mathbf{x}}_{k|k}$ and the corresponding error covariance matrix $\mathbf{P}_{k|k}$ are calculated as follows:

$$
\mathbf{K}_k = \mathbf{P}_{xz,k|k-1} / \mathbf{P}_{zz,k|k-1} \tag{12}
$$

$$
\hat{\mathbf{x}}_{k|k} = \hat{\mathbf{x}}_{k|k-1} + \mathbf{K}_k \left(\mathbf{z}_k - \hat{\mathbf{z}}_{k|k-1}\right) \tag{13}
$$

$$
\mathbf{P}_{k|k} = \mathbf{P}_{k|k-1} - \mathbf{K}_k \mathbf{P}_{zz,k|k-1} \mathbf{K}_k^T \tag{14}
$$

C. PROBLEM STATEMENT

If both the process noise and measurement noise of the dynamic system follow the Gaussian distribution, the conventional CKF-based SINS/GNSS integration will produce the optimal estimation of navigation error when the statistics of the process and measurement noise are accurately known. However, due to the vehicle's severe maneuver, substantial measurement noise of accelerometer and gyro are produced. As a result, the statistic of SINS/GNSS integrated navigation system process noise may be time-variant and inaccurate. Furthermore, due to the abnormal measurement of GNSS, the Gaussian assumption may not always hold in practical application. As a result, the sigma points of the conventional

CKF may not capture the true statistics of the navigation error, resulting in poor or even severely degraded estimation performance. Thus, the statistic of SINS/GNSS integrated navigation system process noise may be unknown and the measurement noise may not follow the Gaussian distribution in the case of the vehicle's severe maneuver and abnormal measurement of GNSS, which will significantly degrade the performance of the conventional CKF-based SINS/GNSS integrated navigation. The aforementioned challenges represent the main motivation for this work.

III. PROPOSED AGMC-CKF

The proposed AGMC-CKF is developed in the following three major steps, namely a batch-mode regression form step, a robust state estimation step and a parameter determination step. Then, some practical implementation issues are discussed.

A. DERIVATION OF THE PROPOSED AGMC-CKF

Given the estimated state vector $\hat{\mathbf{x}}_{k-1|k-1}$ and the corresponding covariance matrix $\mathbf{P}_{k-1|k-1}$ at time step k-1, the predicted state vector $\hat{\mathbf{x}}_{k|k-1}$ along with its covariance matrix $\mathbf{P}_{k|k-1}$ can be obtained through (5) and (6). To derive the batch-mode linear regressive form, we define the prior estimation error of the state by $\delta_k = \mathbf{x}_k - \hat{\mathbf{x}}_{k|k-1}$, where $E\left[\delta_k\delta_k^T\right] = \mathbf{P}_{k|k-1}$, $\mathbf{x}_k$ is the true state vector and $\hat{\mathbf{x}}_{k|k-1}$ is the predicted state vector. Then applying the statistic linearization to the nonlinear observation equation around $\hat{\mathbf{x}}_{k|k-1}$, yielding:

$$\mathbf{z}_k = \hat{\mathbf{z}}_{k|k-1} + \tilde{\mathbf{H}}_k\left(\hat{\mathbf{x}}_k - \hat{\mathbf{x}}_{k|k-1}\right) + \eta_k + \mathbf{v}_k \quad (15)$$

where $\tilde{\mathbf{H}}_k = \left(\mathbf{P}_{xz,k|k-1}\right)^T\mathbf{P}_{k|k-1}^{-1}$ is the measurement slope matrix, η_k is the statistical linearization error term which is used to compensate the high order Taylor-series expansion error. The covariance matrix of η_k is calculated as:

$$\hat{\mathbf{R}}_k = E\left[\eta_k\eta_k^T\right] = \mathbf{P}_{zz,k|k-1} - \left(\mathbf{P}_{xz,k|k-1}\right)^T\mathbf{P}_{k|k-1}^{-1}\mathbf{P}_{xz,k|k-1} \quad (16)$$

In order to handle the predicted state vector and received measurements simultaneously, we construct the batch-mode linear regression form as follows:

$$\begin{bmatrix}\hat{\mathbf{x}}_{k|k-1} \\ \tilde{\mathbf{z}}_k\end{bmatrix} = \begin{bmatrix}\mathbf{I} \\ \tilde{\mathbf{H}}_k\end{bmatrix}\mathbf{x}_k + \begin{bmatrix}-\delta_k \\ \eta_k + \mathbf{v}_k\end{bmatrix} \quad (17)$$

where $\tilde{\mathbf{z}}_k = \mathbf{z}_k - \hat{\mathbf{z}}_{k|k-1} + \tilde{\mathbf{H}}_k\hat{\mathbf{x}}_{k|k-1}$, the batch-mode regression form in (17) can be written in the compact form as follows:

$$\bar{\mathbf{z}}_k = \bar{\mathbf{H}}_k\mathbf{x}_k + \bar{\varepsilon}_k \quad (18)$$

where $\bar{\varepsilon}_k = \begin{bmatrix}-\delta_k \\ \eta_k + \mathbf{v}_k\end{bmatrix}$, and the corresponding error covariance matrix $\mathbf{W}_k$ is given by

$$\mathbf{W}_k = E\left[\bar{\varepsilon}_k\bar{\varepsilon}_k^T\right] = \begin{bmatrix}\mathbf{P}_{k|k-1} & 0 \\ 0 & \sum_k\end{bmatrix}$$
$$= \begin{bmatrix}\mathbf{S}_{p,k|k-1}\mathbf{S}_{p,k|k-1}^T & 0 \\ 0 & \mathbf{S}_{\Sigma,k}\mathbf{S}_{\Sigma,k}^T\end{bmatrix}$$
$$= \mathbf{S}_k\mathbf{S}_k^T \quad (19)$$

where $\sum_k = E\left[\left(\eta_k + \mathbf{v}_k\right)\left(\eta_k + \mathbf{v}_k\right)^T\right] = \mathbf{R}_k + \hat{\mathbf{R}}_k$, $\mathbf{S}_k$ can be obtained by the Cholesky decomposition of $\mathbf{W}_k$. To uncorrelated the predicted state vector and measurement vector, we multiply both sides of (18), yielding:

$$\mathbf{S}_k^{-1}\bar{\mathbf{z}}_k = \mathbf{S}_k^{-1}\bar{\mathbf{H}}_k\mathbf{x}_k + \mathbf{S}_k^{-1}\bar{\varepsilon}_k \quad (20)$$

Then the batch-mode regression form can be further transformed to

$$\mathbf{D}_k = g\left(\mathbf{x}_k\right) + \xi_k \quad (21)$$

where $\mathbf{D}_k = \mathbf{S}_k^{-1}\bar{\mathbf{z}}_k$, $g\left(\mathbf{x}_k\right) = \mathbf{S}_k^{-1}\bar{\mathbf{H}}_k\mathbf{x}_k$ and $\xi_k = \mathbf{S}_k^{-1}\bar{\varepsilon}_k$. It can be easily verified that $E\left[\xi_k\xi_k^T\right] = \mathbf{I}$.

To make the filtering robust to the non-gaussian noise, we introduce the concept of maximum correntropy based on the above batch-mode regression model. The definition of maximum correntropy can be referred to Appendix A. Motivated by the maximum correntropy and weighted least square method, we proposed in this paper a new criterion termed adaptive generalized maximum correntropy criterion (AGMC) as follows:

$$J_{AGMC}\left(x_k\right) = \left\|\mathbf{x}_k - \hat{\mathbf{x}}_{k|k-1}\right\|_{\left(\lambda_k\mathbf{p}_{k|k-1}\right)^{-1}}^2 - \sum_{i=n}^{m}\rho_{GMC}\left(\mathbf{e}_{k,i}\right) \quad (22)$$

where $\|x\|_A^2 = x^TAx$ is the quadratic form with respect to A. λ_k is the fading factor, which is used to adaptively adjust the predicted error covariance matrix and strengthen the robustness of the proposed filter against the unknown process noise. $\mathbf{e}_{k,i} = \mathbf{D}_{k,i} - g\left(\mathbf{x}_{k,i}\right)$, $\mathbf{e}_{k,i}$ is the i-th element of $\mathbf{e}_k$, n and m are respectively the dimension of $\mathbf{x}_k$ and $\mathbf{D}_k$. $\rho_{GMC}\left(\mathbf{e}_{k,i}\right)$ is the kernel function of the correntropy. Due to the fact that the correntropy with the standard Gaussian kernel is not always the best in practical application, we adopt in this paper the following generalized Gaussian density function as the kernel function:

$$\rho_{GMC}\left(\mathbf{e}_{k,i}\right) = \frac{\alpha}{2\beta\Gamma\left(1/\alpha\right)}\exp\left(-\beta^{-\alpha}\mathbf{e}_{k,i}^{\alpha}\right) \quad (23)$$

where α is the shape parameter, β is the bandwidth parameter. As can be seen from (23) that the original correntropy with the Gaussian kernel is a special case of the generalized Gaussian kernel when $\alpha = 2$ and $\beta = \sqrt{2}\sigma$.

Under the adaptive generalized maximum correntropy criterion defined above, we develop a new robust CKF and obtain the optimal solution of $\mathbf{x}_k$ by minimizing the following objective function as follows:

$$\hat{\mathbf{x}}_k = \arg\min_{\mathbf{x}_k}J_{AGMC}\left(x_k\right) \quad (24)$$

Thus, the solution of (24) can be obtained by differencing the cost function with respect to $\mathbf{x}_k$ and setting it equal to zero as follows:

$$\left(\lambda_k\mathbf{P}_{k|k-1}\right)^{-1}\left(\mathbf{x}_k - \hat{\mathbf{x}}_{k|k-1}\right) - \sum_{i=n}^{m}\psi\left(\mathbf{e}_{k,i}\right)\frac{\partial\mathbf{e}_{k,i}}{\partial\mathbf{x}_k} = 0 \quad (25)$$

where $\psi\left(\mathbf{e}_{k,i}\right) = \frac{\partial \rho_{GMC}\left(\mathbf{e}_{k,i}\right)}{\partial \mathbf{e}_{k,i}} = -\frac{\alpha^2 \mathbf{e}_{k,i}^{\alpha-1}}{2\beta^{\alpha+1}\Gamma(1/\alpha)} \exp\left(-\beta^{-\alpha}\mathbf{e}_{k,i}^{\alpha}\right)$, by defining the function $\mathbf{C}_{k,i} = -\frac{\alpha^2 \mathbf{e}_{k,i}^{\alpha-2}}{2\beta^{\alpha+1}\Gamma(1/\alpha)} \exp\left(-\beta^{-\alpha}\mathbf{e}_{k,i}^{\alpha}\right)$ and dialog matrix $\mathbf{C}_k = diag\left[\mathbf{C}_{k,i}\right] i = n, \cdots, m$, we can rewrite equation (25) as follows:

$$\left(\lambda_k \mathbf{P}_{k|k-1}\right)^{-1}\left(\mathbf{x}_k - \hat{\mathbf{x}}_{k|k-1}\right) - \tilde{\mathbf{H}}^T \mathbf{S}_{\Sigma,k}^{-T}\mathbf{C}_k\mathbf{e}_k = 0 \quad (26)$$

Substituting $\mathbf{e}_k = \mathbf{D}_k - g\left(\mathbf{x}_k\right) = \mathbf{S}_{\Sigma,k}^{-1}\left(\tilde{\mathbf{z}}_k - \tilde{\mathbf{H}}_k\mathbf{x}_k\right)$ into (26) yields:

$$\left(\lambda_k \mathbf{P}_{k|k-1}\right)^{-1}\left(\mathbf{x}_k - \hat{\mathbf{x}}_{k|k-1}\right) - \tilde{\mathbf{H}}_k^T \mathbf{S}_{\Sigma,k}^{-T}\mathbf{C}_k\mathbf{S}_{\Sigma,k}^{-1}$$
$$\times \left(\tilde{\mathbf{z}}_k - \tilde{\mathbf{H}}_k\mathbf{x}_k\right) = 0 \quad (27)$$

Let $\bar{\mathbf{P}}_{k|k-1} = \lambda_k \mathbf{P}_{k|k-1}$, $\bar{\mathbf{R}}_k = \mathbf{S}_{\Sigma,k}\mathbf{C}_k^{-1}\mathbf{S}_{\Sigma,k}^T$ and $\hat{\mathbf{x}}_{k|k} = \mathbf{x}_k$ it can be obtained that:

$$\bar{\mathbf{P}}_{k|k-1}^{-1}\left(\hat{\mathbf{x}}_{k|k} - \hat{\mathbf{x}}_{k|k-1}\right) = \tilde{\mathbf{H}}_k^T \bar{\mathbf{R}}_k^{-1}\left(\tilde{\mathbf{z}}_k - \tilde{\mathbf{H}}_k\hat{\mathbf{x}}_{k|k}\right) \quad (28)$$

By adding and subtracting the term $\tilde{\mathbf{H}}_k^T \bar{\mathbf{R}}_k^{-1}\tilde{\mathbf{H}}_k\hat{\mathbf{x}}_{k|k-1}$ on the right side of (28) it can be acquired that:

$$\left(\bar{\mathbf{P}}_{k|k-1}^{-1} + \tilde{\mathbf{H}}_k^T \bar{\mathbf{R}}_k^{-1}\tilde{\mathbf{H}}_k\right)\hat{\mathbf{x}}_{k|k} = \bar{\mathbf{P}}_{k|k-1}^{-1}\hat{\mathbf{x}}_{k|k-1} + \tilde{\mathbf{H}}_k^T \bar{\mathbf{R}}_k^{-1}\tilde{\mathbf{z}}_k$$
$$-\tilde{\mathbf{H}}_k^T \bar{\mathbf{R}}_k^{-1}\tilde{\mathbf{H}}_k\hat{\mathbf{x}}_{k|k-1} + \tilde{\mathbf{H}}_k^T \bar{\mathbf{R}}_k^{-1}\tilde{\mathbf{H}}_k\hat{\mathbf{x}}_{k|k-1} \quad (29)$$

$$\left(\bar{\mathbf{P}}_{k|k-1}^{-1} + \tilde{\mathbf{H}}_k^T \bar{\mathbf{R}}_k^{-1}\tilde{\mathbf{H}}_k\right)\hat{\mathbf{x}}_{k|k} = \left(\bar{\mathbf{P}}_{k|k-1}^{-1} + \tilde{\mathbf{H}}_k^T \bar{\mathbf{R}}_k^{-1}\tilde{\mathbf{H}}_k\right)\hat{\mathbf{x}}_{k|k-1}$$
$$+\tilde{\mathbf{H}}_k^T \bar{\mathbf{R}}_k^{-1}\left(\tilde{\mathbf{z}}_k - \tilde{\mathbf{H}}_k\hat{\mathbf{x}}_{k|k-1}\right) \quad (30)$$

Then, left multiply both sides of (30) by $(\bar{\mathbf{P}}_{k|k-1}^{-1} + \tilde{\mathbf{H}}_k^T \bar{\mathbf{R}}_k^{-1}\tilde{\mathbf{H}}_k)^{-1}$ to obtain the following results:

$$\hat{\mathbf{x}}_{k|k} = \hat{\mathbf{x}}_{k|k-1} + \mathbf{K}_k\left(\mathbf{z}_k - \hat{\mathbf{z}}_{k|k-1}\right) \quad (31)$$

$$\mathbf{K}_k = \left(\bar{\mathbf{P}}_{k|k-1}^{-1} + \tilde{\mathbf{H}}_k^T \bar{\mathbf{R}}_k^{-1}\tilde{\mathbf{H}}_k\right)^{-1}\tilde{\mathbf{H}}_k^T \bar{\mathbf{R}}_k^{-1} \quad (32)$$

Meanwhile, the corresponding posterior covariance matrix can be updated by:

$$\bar{\mathbf{P}}_{k|k} = \left(\mathbf{I} - \mathbf{K}_k\tilde{\mathbf{H}}_k\right)\bar{\mathbf{P}}_{k|k-1}\left(\mathbf{I} - \mathbf{K}_k\tilde{\mathbf{H}}_k\right)^T + K_k\bar{\mathbf{R}}_k K_k^T$$
$$= \left(\mathbf{I} - \mathbf{K}_k\tilde{\mathbf{H}}_k\right)\bar{\mathbf{P}}_{k|k-1} \quad (33)$$

It can be observed from the above equations that the fading factor λ_k is the unknown parameter to be determined in the process of dealing with uncertain process noise. In this paper, we proposed an adaptive forgetting scheme to estimate the fading factor adaptively. The basic idea of the adaptive forgetting scheme is to update the fading factor by using the empirically estimated residual covariance via the recursive least squares (RLS) algorithm. Specifically, we can obtain the innovation covariance matrix as follows:

$$\mathbf{P}_{zz,k|k-1} = \mathbf{H}_k\bar{\mathbf{P}}_{k|k-1}\mathbf{H}_k^T + \bar{\mathbf{R}}_k \quad (34)$$

where $\bar{\mathbf{P}}_{k|k-1} = \lambda_k \mathbf{P}_{k|k-1}, \bar{\mathbf{R}}_k = \mathbf{S}_{\Sigma,k}\mathbf{C}_k^{-1}\mathbf{S}_{\Sigma,k}^T$, which are different from the normal covariance matrix denoted by $\mathbf{P}_{k|k-1}$ and $\mathbf{R}_k$ due to the time-varying process noise and

non-Gaussian measurement noise. By substituting $\bar{\mathbf{P}}_{k|k-1} = \lambda_k \mathbf{P}_{k|k-1}$ into (34), we get:

$$\mathbf{P}_{zz,k|k-1} = \lambda_k \mathbf{H}_k\mathbf{P}_{k|k-1}\mathbf{H}_k^T + \bar{\mathbf{R}}_k \quad (35)$$

By taking the trace on both sides of (35), yielding:

$$trace\left(\mathbf{P}_{zz,k|k-1}\right) = \lambda_k trace\left(\mathbf{H}_k\mathbf{P}_{k|k-1}\mathbf{H}_k^T\right) + trace\left(\bar{\mathbf{R}}_k\right) (36)$$

The innovation covariance matrix $\mathbf{P}_{zz,k|k-1}$ can also be estimated empirically by using the innovations in a fixed-width moving window under the assumption that the innovations are stationary:

$$\hat{\mathbf{P}}_{zz,k|k-1} = \frac{1}{M}\sum_{i=0}^{M-1}\mathbf{e}_{k-i}\mathbf{e}_{k-i}^T \quad (37)$$

where M is the width of the moving window for estimating the innovation covariance matrix. On one hand, if M is too large, the proposed AGMC-CKF will suffer from a severe computational burden. On the other hand, if M is too small, it may yield large innovation variance. In this paper, the window width is determined by minimizing the variance parameters according to [29]. $\mathbf{e}_k = \mathbf{z}_k - \hat{\mathbf{z}}_{k|k-1}$ denotes the innovation matrix. Thus, the optimal estimation of the fading factor λ_k can be reduced to the linear regressive problem as follows:

$$trace\left(\hat{\mathbf{P}}_{zz,k|k-1}\right) \approx \lambda_k trace\left(\mathbf{H}_k\mathbf{P}_{k|k-1}\mathbf{H}_k^T\right) + trace\left(\bar{\mathbf{R}}_k\right) \quad (38)$$

To solve the linear regressive problem recursively, we propose to use the recursive least squares (RLS) algorithm to efficiently produce the optimal estimation of λ_k online with the following measurement model:

$$\mathbf{y}_k^\lambda = \mathbf{H}_k^\lambda\mathbf{x}_k^\lambda + \mathbf{v}_k^\lambda \quad (39)$$

where $\mathbf{y}_k^\lambda = trace\left(\hat{\mathbf{P}}_{zz,k|k-1}\right) - trace\left(\bar{\mathbf{R}}_k\right)$ is the measurement vector, $\mathbf{x}_k^\lambda = \lambda_k$, $\mathbf{H}_k^\lambda = trace\left(\mathbf{H}_k\mathbf{P}_{k|k-1}\mathbf{H}_k^T\right)$, $\mathbf{v}_k^\lambda$ is the zero-mean random vector with the variance matrix $\mathbf{R}_k^\lambda$. By utilizing the RLS, the fading factor λ_k at the k-1 iteration can be calculated through

$$\hat{\mathbf{x}}_k^\lambda = \hat{\mathbf{x}}_{k-1}^\lambda + \mathbf{K}_k^\lambda\left(\mathbf{y}_k^\lambda - \hat{\mathbf{y}}_k^\lambda\right) \quad (40)$$

where $\mathbf{K}_k^\lambda = \mathbf{P}_{k-1}^\lambda\left(\mathbf{H}_k^\lambda\right)^T\left(\mathbf{R}_k^\lambda + \mathbf{H}_k^\lambda\mathbf{P}_{k-1}^\lambda\left(\mathbf{H}_k^\lambda\right)^T\right)^{-1}$, $\mathbf{P}_k^\lambda = \left(\mathbf{I} - \mathbf{K}_m^\lambda\mathbf{H}_m^\lambda\right)\mathbf{P}_{k-1}^\lambda$, $\hat{\mathbf{y}}_k^\lambda = \mathbf{H}_k^\lambda\hat{\mathbf{x}}_{k-1}^\lambda$.

B. PRACTICAL IMPLEMENTATION ISSUES OF THE PROPOSED AGMC-CKF

1) OUTLIER IDENTIFYING

It is worth noting that the measurement noise covariance matrix $\bar{\mathbf{R}}_k = \mathbf{S}_{\Sigma,k}\mathbf{C}_k^{-1}\mathbf{S}_{\Sigma,k}^T$ in the proposed AGMC-CKF depends largely on the calculation of $\mathbf{C}_k^{-1}$. However, if the outlier occurs, the inversion matrix of $\mathbf{C}_k$ may not exist, that is when $\|\mathbf{z}_k\| \to \infty$, $\mathbf{C}_{k,i} \to 0$, $\mathbf{C}_k = diag\left[\mathbf{C}_{k,i}\right] \to 0$. To overcome this problem, we first detect the outliers using the hypotheses test method, in which the square of the

Mahalanobis distance from the predicted residual vector is used as the test statistic:

$$\boldsymbol{\gamma}_k = M_k^2 = \mathbf{e}_k^T \left[\lambda_k \mathbf{H}_k \mathbf{P}_{k|k-1} \mathbf{H}_k^T + \bar{\mathbf{R}}_k \right]^{-1} \mathbf{e}_k \quad (41)$$

where $\mathbf{e}_k = \mathbf{z}_k - \hat{\mathbf{z}}_{k|k-1}$ is the predicted residual, $M_k = \sqrt{\mathbf{e}_k^T \left[\lambda_k \mathbf{H}_k \mathbf{P}_{k|k-1} \mathbf{H}_k^T + \bar{\mathbf{R}}_k \right]^{-1} \mathbf{e}_k}$ is the Mahalanobis distance of the predicted residual $\mathbf{e}_k$. Since $\mathbf{e}_k$ is a random variable roughly obeying the Gaussian distribution, the square of the Mahalanobis distance of the predicted residual should follow the χ^2 distribution with m-degree of freedom (m is the number of state variables that can be directly observed). According to the hypothesis testing theory, for a chosen significance level α, we have

$$P \left(\chi^2 < \chi_{\alpha,\mathrm{m}}^2 \right) = 1 - \alpha \quad (42)$$

where $P(\cdot)$ denotes the probability of a random event. The $\chi_{\alpha,\mathrm{m}}^2$ of the Chi-square distribution is predetermined as $\chi_{\alpha,\mathrm{m}}^2 = 12.592$ with the significance level at 5%. So if the actual γ_k is lower than this α-quantile, i.e. $\gamma_k < \chi_{\alpha,\mathrm{m}}^2$, which means that there is no measurement outlier existed, and then both the time update and measurement update in the proposed AGMC-CKF are carried out. Otherwise, it can be concluded with high probability $(1 - \alpha)$ that there exists a measurement outlier in the dynamic system. To avoid the matrix $\mathbf{C}_k$ being nearly singular, only the time update of the AGMC-CKF is conducted under this condition. With the outlier identification, the numerical problem when calculating the inversion matrix of $\mathbf{C}_k$ can be effectively avoided.

2) PARAMETER SELECTION

To implement the proposed AGMC-CKF, several parameters need to be selected, namely the setting of the kernel parameters α and β of the adaptive generalized maximum correntropy criterion and the covariance matrix $\mathbf{R}$ of the RLS algorithm. Regarding the kernel parameters α and β, they determine the robustness of AGMC and are generally selected by trial in practical application since they are related to the practical environment. On one hand, if the kernel parameters are too large, the AGMC will be insensitive to some outliers and even the AGMC-CKF reduced to the conventional CKF when $\beta \to \infty$. On the other hand, when the kernel parameters are too small, the contribution of the useful information will be ignored, which may result in degraded performance and even lead to filtering divergence. To find the optimal kernel parameters and investigate how the kernel parameters affect the filtering accuracy of the proposed AGMC-CKF, we evaluated the several values of the kernel parameters by experience according to the special environment in different applications. The optimal determined kernel parameters are provided in the simulation and experiment section. $\mathbf{R}_k^\lambda$ is the measurement error covariance matrix in the measurement model as shown in (39), which determines the weight between the recent measurement data and the predicted state. Regarding the covariance matrix $\mathbf{R}_k^\lambda$ of the RLS algorithm, a smaller $\mathbf{R}_k^\lambda$

will put more emphasis on the recent measurement data; in contrast, a large $\mathbf{R}_k^\lambda$ will discount the recent data and rely more on the predicted state for state estimation. Extensive simulations have shown that the covariance matrix $\mathbf{R}_k^\lambda$ can be set to 0.01 to achieve a good estimation performance.

3) COMPUTATIONAL EFFICIENCY IMPROVEMENT

Another important problem that needs to be addressed in the practical implementation of the proposed AGMC-CKF is how to reduce the computational complexity. We can notice from the expression (32) for the calculation of the Kalman filter that two $n \times n$ and one $m \times m$ inversion matrix calculation are required, since $\bar{\mathbf{P}}_{k|k-1} \in \mathbb{R}^{n \times n}$, $\left(\bar{\mathbf{P}}_{k|k-1}^{-1} + \tilde{\mathbf{H}}_k^T \bar{\mathbf{R}}_k^{-1} \tilde{\mathbf{H}}_k \right)^{-1} \in \mathbb{R}^{n \times n}$ and $\bar{\mathbf{R}}_k \in \mathbb{R}^{m \times m}$, which may leads to large computational burden in the proposed AGMC-CKF, especially for the high-dimensional SINS/GNSS integrated navigation system. To address this issue, we propose to modify the Kalman gain in (32) as an alternate form as follows:

Similar to the measurement update of classical KF, we can prove that the following formulas hold [6]:

$$\mathbf{K}_k = \left(\bar{\mathbf{P}}_{k|k-1}^{-1} + \tilde{\mathbf{H}}_k^T \bar{\mathbf{R}}_k^{-1} \tilde{\mathbf{H}}_k \right)^{-1} \tilde{\mathbf{H}}_k^T \bar{\mathbf{R}}_k^{-1} = \bar{\mathbf{P}}_{k|k} \tilde{\mathbf{H}}_k^T \bar{\mathbf{R}}_k^{-1} \quad (43)$$

Substituting (33) into (43) gives:

$$\mathbf{K}_k = \left(\mathbf{I} - \mathbf{K}_k \tilde{\mathbf{H}}_k \right) \bar{\mathbf{P}}_{k|k-1} \tilde{\mathbf{H}}_k^T \bar{\mathbf{R}}_k^{-1} \quad (44)$$

$$\mathbf{K}_k \left(\mathbf{I} + \tilde{\mathbf{H}}_k \bar{\mathbf{P}}_{k|k-1} \tilde{\mathbf{H}}_k^T \bar{\mathbf{R}}_k^{-1} \right) = \bar{\mathbf{P}}_{k|k-1} \tilde{\mathbf{H}}_k^T \bar{\mathbf{R}}_k^{-1} \quad (45)$$

With $\mathbf{I} = \bar{\mathbf{R}}_k \bar{\mathbf{R}}_k^{-1}$, (45) can be transformed to the form as follows:

$$\mathbf{K}_k \left(\bar{\mathbf{R}}_k + \tilde{\mathbf{H}}_k \bar{\mathbf{P}}_{k|k-1} \tilde{\mathbf{H}}_k^T \right) \bar{\mathbf{R}}_k^{-1} = \bar{\mathbf{P}}_{k|k-1} \tilde{\mathbf{H}}_k^T \bar{\mathbf{R}}_k^{-1} \quad (46)$$

$$\mathbf{K}_k = \frac{\bar{\mathbf{P}}_{k|k-1} \tilde{\mathbf{H}}_k^T}{\bar{\mathbf{R}}_k + \tilde{\mathbf{H}}_k \bar{\mathbf{P}}_{k|k-1} \tilde{\mathbf{H}}_k^T} \quad (47)$$

In contrast to the conventional form for $\mathbf{K}_k$ in (32), the alternate form in (47) requires only one matrix inversion, which greatly improves the computational efficiency of the proposed AGMC-CKF for the high-dimensional SINS/GNSS integrated navigation system.

C. SUMMARY OF THE PROPOSED AGMC-CKF

The implementation pseudocode for the proposed AGMC-CKF algorithm is presented as Alogritm1.

IV. PERFORMANCE EVALUATION

In this section, the car-mounted experiment is carried out to assess the performance of the proposed AGMC-CKF. To further verify the effectiveness and superiority of the proposed AGMC-CKF, some representative state-of-the-art approaches such as the cubature Kalman filter (CKF), robust Student's t-based nonlinear filter (RSTNF) and Strong tracking maximum correntropy cubature Kalman filter (MCCKF) are used for comparison.

Algorithm 1 One Time Step of the Proposed AGMC-CKF Algorithm

Initialization: $\hat{\mathbf{x}}_{0|0}, \bar{\mathbf{P}}_{0|0},$

1. Compute the predicted state vector $\hat{\mathbf{x}}_{k|k-1}$ and the corresponding error covariance matrix $\mathbf{P}_{k|k-1}$ using (5) - (11);

2. Identify the outlier according to (41)-(42). If the outliers existed, $\hat{\mathbf{x}}_{k|k} = \hat{\mathbf{x}}_{k|k-1}, \bar{\mathbf{P}}_{k|k} = \mathbf{P}_{k|k-1}, k = k+1$ and go back to step 1; else go to step 3;

3. Calculate $\mathbf{S}_k$ by applying Cholesky decomposition $\mathbf{W}_k = \mathbf{S}_k \mathbf{S}_k^T$;

4. Calculate $\mathbf{e}_{k,i}$ using $\mathbf{e}_{k,i} = \mathbf{D}_{k,i} - g(\mathbf{x}_{k,i})$ where $\mathbf{D}_k = \mathbf{S}_k^{-1}\bar{\mathbf{z}}_k, g(\mathbf{x}_k) = \mathbf{S}_k^{-1}\bar{\mathbf{H}}_k\mathbf{x}_k$;

5. Calculate $\mathbf{C}_k$ using $\mathbf{C}_k = diag[\mathbf{C}_{k,i}] i = 1, \cdots, m,$ where $\mathbf{C}_{k,i} = -\frac{\alpha^2 \mathbf{e}_{k,i}^{\alpha-2}}{2\beta^{\alpha+1}\Gamma(1/\alpha)} \exp\left(-\beta^{-\alpha}\mathbf{e}_{k,i}^\alpha\right)$;

6. Calculate $\bar{\mathbf{R}}_k$ using $\bar{\mathbf{R}}_k = \mathbf{S}_k \mathbf{C}_k^{-1} \mathbf{S}_k^T$;

7. Calculate the fading factor λ_k using (35)~(40);

8. $\bar{\mathbf{P}}_{k|k-1} = \lambda_k \mathbf{P}_{k|k-1}$

9. $\mathbf{K}_k = \frac{\bar{\mathbf{P}}_{k|k-1}\mathbf{H}_k^T}{\bar{\mathbf{R}}_k + \mathbf{H}_k\bar{\mathbf{P}}_{k|k-1}\mathbf{H}_k^T}$

$\hat{\mathbf{x}}_{k|k} = \hat{\mathbf{x}}_{k|k-1} + \mathbf{K}_k\left(\mathbf{z}_k - \mathbf{H}_k\hat{\mathbf{x}}_{k|k-1}\right)$

$\bar{\mathbf{P}}_{k|k} = (\mathbf{I} - \mathbf{K}_k\mathbf{H}_k)\bar{\mathbf{P}}_{k|k-1}(\mathbf{I} - \mathbf{K}_k\mathbf{H}_k)^T + \mathbf{K}_k\bar{\mathbf{R}}_k\mathbf{K}_k^T = (\mathbf{I} - \mathbf{K}_k\mathbf{H}_k)\bar{\mathbf{P}}_{k|k-1}$

Output: $\hat{\mathbf{x}}_{k|k}, \bar{\mathbf{P}}_{k|k}$

A. NOISE STATISTICAL MODEL OF LOOSE SINS/GNSS

For the loosely coupled SINS/GNSS nonlinear model in equation (2), $\mathbf{v}_{k-1} \sim N(0, \mathbf{Q}_k)$ denotes the process noise, which is assumed to be white and independent of each other. Under the condition of vehicle's severe maneuvering, $\mathbf{Q}_k = diag([\mathbf{n}_g^2, \mathbf{n}_f^2, \mathbf{n}_{g\delta b}^2, \mathbf{n}_{f\delta b}^2])$ is the time-varying process noise covariance matrix with $\mathbf{n}_g, \mathbf{n}_f, \mathbf{n}_{g\delta b}, \mathbf{n}_{f\delta b}$ being respectively the power spectral density (PSD) of the gyroscope random noise, accelerometer random noise, gyroscope dynamic bias and the accelerometer dynamic bias. The simulation of the time-varing process noise can be shown in the number simulations part.

For the loosely coupled SINS/GNSS measurement model, $\mathbf{v}_k$ is the non-Gaussian measurement noise under the condition of abnormal GNSS measurement, which can be generated according to the mix-Gaussian distribution described in [30] as follows:

$$\mathbf{v}_k \sim (1 - \varepsilon) N(\mathbf{0}, \mathbf{R}_k) + \varepsilon N(\mathbf{0}, 100\mathbf{R}_k) \qquad (48)$$

where $\mathbf{R}_k$ is the nominal covariance matrix from the Gaussian distribution, ε denotes the level of the non-Gaussian contamination, which means that $100(1 - \varepsilon)$ percent of normal values modeled as zero-mean Gaussian distribution and 100ε percent of measurement noise are drawn from the Gaussian distribution with severely increased covariance.

B. NUMERICAL SIMULATIONS

In this section, we carry out extensive simulations on the SINS/GNSS integrated navigation system to demonstrate the
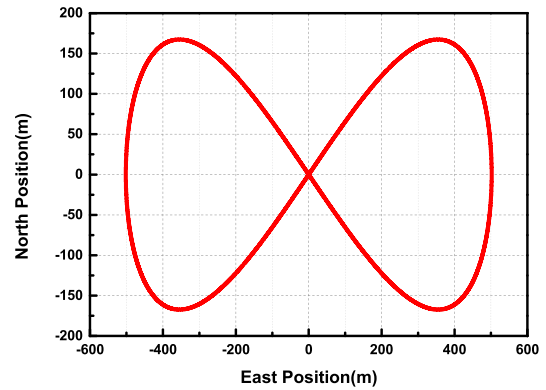

FIGURE 1. Simulation trajectory of the SINS/GNSS.

performance of the proposed AGMC-CKF subjected to various types of unknown noise. Specially, the true trajectory of the SINS/GNSS integrated navigation system is shown in Figure 1. The constant bias of gyroscope and accelerometer are respectively 12 °/h and 5mg. The random noise of gyroscope and accelerometer are respectively $0.6°/\sqrt{h}$ and $0.002m/s^2/\sqrt{h}$. The position and velocity error of GNSS are respectively 1m and 0.1m/s. The update rate of IMU and GNSS are respectively 100Hz and 10Hz. The existing CKF [28], strong tracking Maximum correntropy cubature Kalman filter (MCCKF) [31] and robust student's t based nonlinear filter (RSTNF) [21] are taken into comparison to verify the superiority of the proposed AGMC-CKF. All the filers are configured with identical parameters such as initial state and initial covariance. In the MCCFK, the kernel bandwidth is set as $\sigma = 3$. In the RSTNF, the dof parameter, turning parameter and the iteration number are respectively chosen as: $v = 0.5, \tau = 5, N = 10$. The proposed filter and the existing filters are all coded with MATLAB and carried out on a computer with CPU at 2.60GHz, 8Gb memory.

To evaluate the estimation accuracy of the proposed filter and the existing filters, the mean square error (RMSE) of the velocity and position obtained from the SINS/GNSS integrated navigation system that averaged across all time instances is chosen as the performance metric, which is defined as follows:

$$RMSE = \sqrt{\frac{1}{N}\sum_{k=1}^{N}\left(x_k - \hat{x}_k\right)^2} \qquad (49)$$

where N is the total sample number, x_k and $\hat{x}_k$ denote the true value and the estimated value of velocity and position at time k, respectively.

1) SCENARIOS 1: TIME-VARYING PROCESS NOISE

Due to the different maneuvers of vehicle, the process noise $\mathbf{Q}_t$ may vary over time, yielding deviations from nominal values. In such cases, the performance of the SINS/GNSS will be degraded since the process noises are unknown to the integrated filtering. To validate the performance of different methods to the unknown process noise, the process noise are assumed to be Gaussian distributed with zero means

and time-varying covariance matrix, where the actual process noise covariance matrix are respectively magnified to 10 times and 100 times in the time interval (100, 200) and (250, 350), which are set as follows:

$$\mathbf{Q}_t = \begin{cases} \mathbf{Q}_k & 0 \leq \mathrm{k} \leq 100 \\ 10\mathbf{Q}_k & 100 \leq \mathrm{k} \leq 200 \\ \mathbf{Q}_k & 200 \leq \mathrm{k} \leq 250 \\ 100\mathbf{Q}_k & 250 \leq \mathrm{k} \leq 350 \\ \mathbf{Q}_k & 350 \leq \mathrm{k} \leq 405 \end{cases}$$

The velocity RMSEs of the SINS/GNSS integrated navigation system obtained from existing filters and the proposed filter are displayed in Figure 2. We have not presented the result of the position RMSE here owing to the fact that the position estimation is mainly determined by the measurement noise matrix R and not sensitive to the time-varying process noise. It is apparent that the filtering performance of the traditional CKF is significantly disturbed by the bias process noise covariance, resulting in a large velocity RMSE. Although the RSTNF and MCCKF can cope with them, it produces increased biases on the estimates at the time when the time-varying process noise increases severely. By contrast, the proposed AGMC-CKF can deal with the time-varying process noise and produce much less bias then the RSTNF and MCCKF. This is due to the fact that our proposed adaptive forgetting scheme can effectively track the fading factor and is better than the strong tracking method, hence yielding very good estimates.

2) SCENARIOS 2: NON-GAUSSIAN MEASUREMENT NOISE

Due to the occlusion of trees and buildings, the GNSS measurement noise will deviate from the Gaussian distribution and follow the heavy-tailed non-Gaussian distribution. To assess the sensitivity of different methods to the unknown non-Gaussian noise, the non-Gaussian noise is assumed to follow the Gaussian mixture model, that is the 80% measurement data are drawn from the Gaussian distribution with nominal covariance while the left 20% measurement data are contaminated with the severely increased covariance. In this section, we set the increased covariance as 100 $\mathbf{R}_k$ randomly according to the probability of 20%.The RMSEs of velocity and position of the SINS/GNSS integrated navigation system obtained from the existing filters and proposed filter are respectively shown in Figure 3-4. It can be clearly shown in Figure 3-4 that the velocity and position provided by the traditional CKF has larger RMSE as it is unable to filter out the non-Gaussian noise. By contrast, the RSTNF, MCCKF and the proposed AGMC-CKF are capable of dealing with the non-Gaussian noise thanks to their robustness provided by the maximum correntropy technology, variational Bayesian approach and generalized maximum correntropy approach. However, the proposed AGMC-CKF achieves better estimation accuracy than the MCCKF and RSTNF, which indicates that the generalized maximum correntropy approach has better robustness against the heavy-tailed non-Gaussian noise
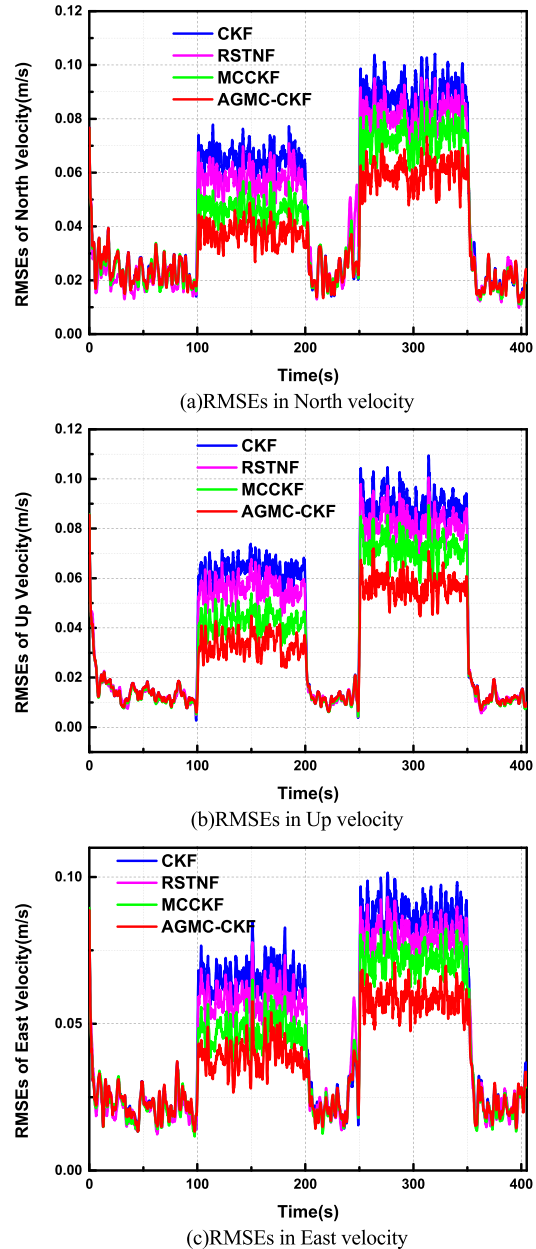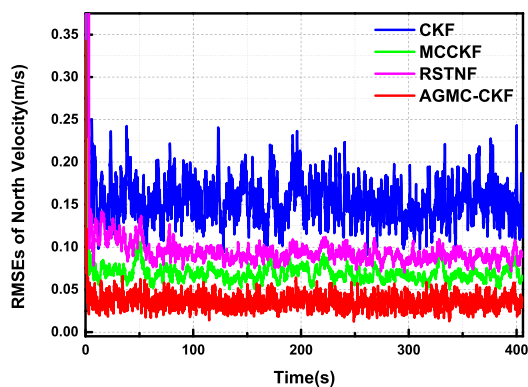

(a)RMSEs in North velocity

(b)RMSEs in Up velocity

(c)RMSEs in East velocity

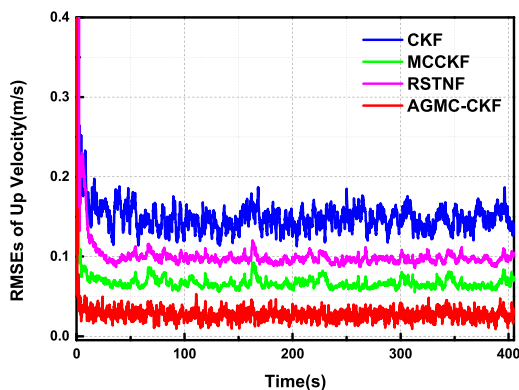**FIGURE 2.** Estimated RMSEs of different filters in scenarios 1.

than the maximum correntropy technology and variational Bayesian approach.

3) COMPUTATIONAL EFFICIENCY

The computational efficiency of the proposed AGMC-CKF is analyzed using MATLAB simulations and compared to that of the existing CKF, MCCKF and RSTNF. The simulations are performed on a PC with intel core i5-3320 CPU at 2.60GHz, 8Gb memory. The single-step running time of each algorithm is utilized to evaluate the computational efficiency. The implementation time of the CKF, MCCKF, RSTNF and the proposed AGMC-CKF for a single-step run in the above two simulation scenarios are presented in Table 1. We can observe from this table that the traditional CKF,

(a)RMSEs in North velocity
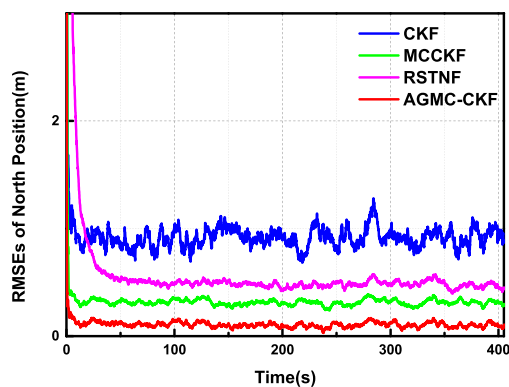

(b)RMSEs in Up velocity
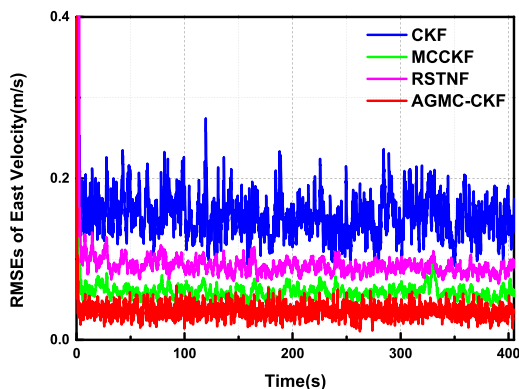
(c)RMSEs in East velocity

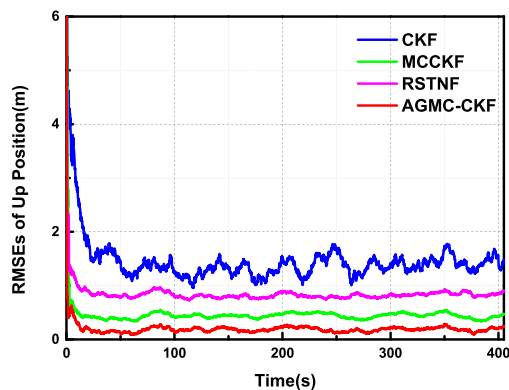**FIGURE 3.** Estimated Velocity RMSEs of different filters in scenarios 2.

(a)RMSEs in North Position

(b)RMSEs in Up Position
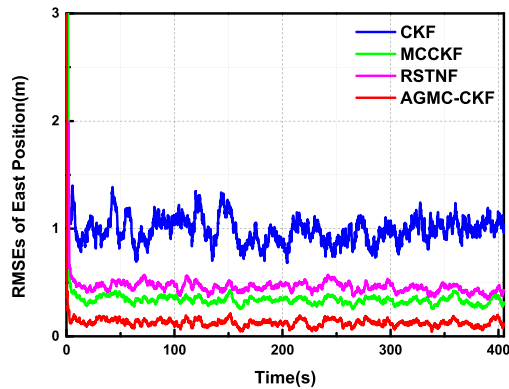
(c)RMSEs in East Position

FIGURE 4. Estimated Position RMSEs of different filters in scenarios 2.

TABLE 1. A single-step running time for the different algorithms.

Scenarios	CKF	MCCKF	RSTNF	AGMC-CKF
Scenario1(ms)	0.406	0.431	0.424	0.436
Scenario2(ms)	0.408	0.432	0.425	0.438

MCCKF and RSTNF have better computational efficiency then the proposed AGMC-CKF, but their state estimation precision is unsatisfied in the above two simulation scenarios. Thus, we can conclude that the proposed AGMC-CKF can achieve better performance with the compromised computational cost when compared with the existing state-of-art methods.

C. CAR-MOUNTED EXPERIMENT

1) EXPERIMENTAL SETUP AND SCENARIOS

In this section, the experimental results are presented to illustrate the effectiveness and superiority of the proposed AGMC-CKF. The car-mounted experimental platform is shown in Figure 5, which is composed of a four-wheeled vehicle equipped with our self-made miniature SINS/GNSS integration navigation system and a high-accuracy reference integration navigation system. In our self-made miniature SINS/GNSS integration navigation system, the sample rate of the GNSS and IMU (inertial measurement unit) data are respectively 10Hz and 1kHz. The dynamic bias of the

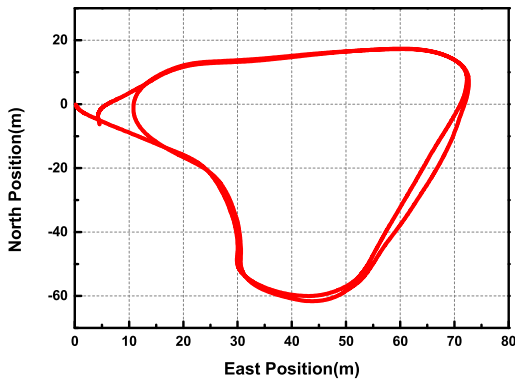**FIGURE 5.** The car-mounted experimental platform.

FIGURE 6. The true trajectory of the vehicle.

FIGURE 7. The angler rate of the vehicle.

FIGURE 8. The acceleration of the vehicle.
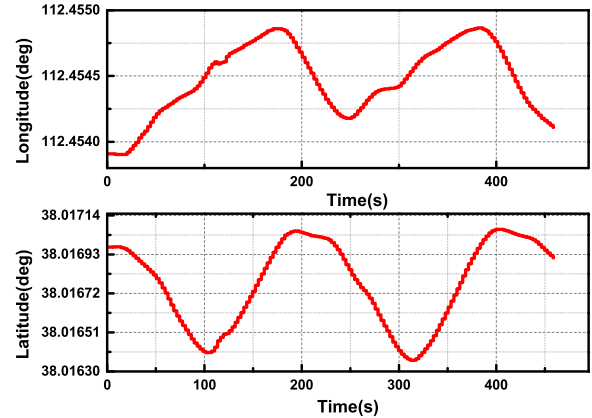
FIGURE 9. The position of the vehicle measured by GNSS.

gyroscope and accelerometer are respectively 12°/h and 5mg. The high-accuracy reference integration navigation system consists of a LCI-1 IMU and a propak satellite receiver, which can provide the reference attitude, velocity and position for performance comparison. For the high-accuracy reference integration navigation, the attitude, velocity and position accuracy are respectively 0.01deg, 0.05m/s and 0.1m. The experiment was carried out in Taiyuan (China), and the total test time is 459s. Figure. 6 demonstrates the true test trajectory. The raw IMU and GPS position information in the experiment are respectively shown in Figure. 7–9. In the car-mounted test, the vehicle maneuvers along a dump road, which produces the time-varying process noise. The IMU measurement and true value influenced by the vehicle vibration in the experiment is shown in Figure. 10. Furthermore, the GNSS always works abnormally due to the occlusion of trees and buildings during the maneuvering, which leads to
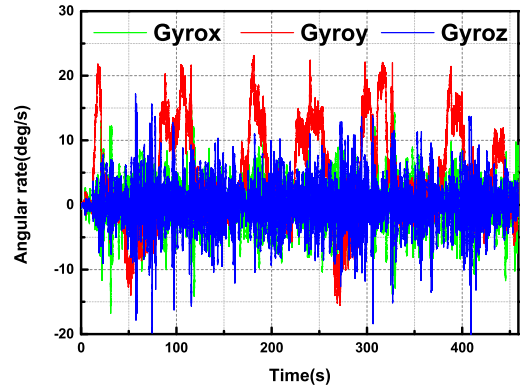
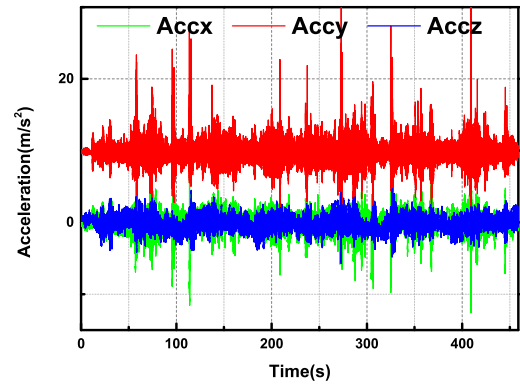the non-Gaussian measurement noise. The error distribution of GNSS velocity measurement in the experiment is shown in Figure. 11. Hence, the car-mounted experiment can be utilized to verify the performance of the proposed AGMC-CKF against the unknown process noise and non-Gaussian measurement noise.

2) PERFORMANCE COMPARISON WITH DIFFERENT ROBUST FILTERING ALGORITHMS

In this section, existing cubature kalman filter (CKF) [28], strong tracking maximum correntropy cubature kalman filter (MCCKF) [31], robust student's t based nonlinear filter (RSTNF) [21] and the proposed AGMC-CKF are tested and
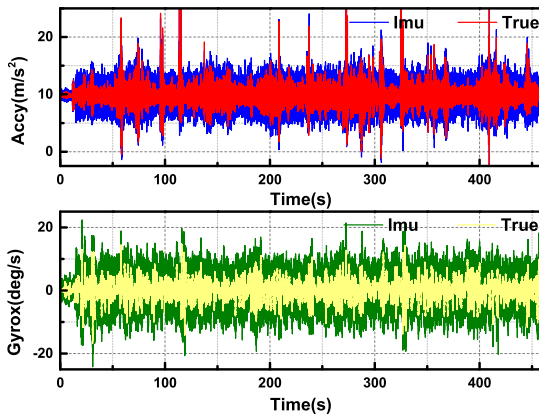
FIGURE 10. The Imu measurement and true value influenced by the vehicle vibration in the experiment.
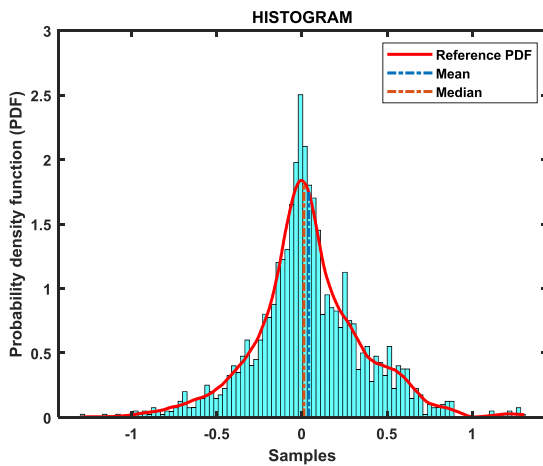

FIGURE 11. The error distribution of GNSS velocity in the experiment.

compared in the car-mounted experiment to evaluate the overall performance of the proposed SINS/GNSS integrated navigation system. In this experiment, the algorithm parameters of the proposed filter and existing filters are respectively set as: The initial state vector and the associated covariance are set as $\hat{x}_{0|0} = \mathbf{0}_{21 \times 1}$ and $\mathbf{P}_{0|0} = $ diag ([0.005rad, 0.015rad, 0.005rad, 0.2m/s, 0.2m/s, 0.2m/s, 10m, 15m, 10m, 0.2deg/s, 0.2deg/s, 0.2deg/s, 16mg, 16mg, 16mg, 0.0018deg/s, 0.0018deg/s, 0.0018deg/s, 0.1mg, 0.1mg, 0.1mg])^2, respectively. The initial value of the nominal process noise covariance matrix and measurement noise covariance matrix are respectively set as $\mathbf{Q}_k = $ diag([0.3deg/sqrt(h), 0.3deg/sqrt(h), 0.3deg/sqrt(h), 0.3m/s^2/sqrt(Hz), 0.3m/s^2/sqrt(Hz), 0.3m/s^2/sqrt(Hz), 0.3 deg/sqrt(h), 0.3deg/sqrt(h), 0.3deg/sqrt(h), 0.3m/s^2/sqrt(Hz), 0.3 m/s^2/sqrt(Hz), 0.3m/s^2/sqrt(Hz)])^2 and $\mathbf{R}_k$ = diag ([0.2m/s, 0.2m/s, 0.2m/s, 10m, 15m, 10m])^2. In the MCCFK, the kernel bandwidth is set as $\sigma = 10$. In the RSTNF, the dof parameter, turning parameter and the iteration number are chosen as: $v = 0.2$, $\tau = 5$ and $N = 5$. In our proposed AGMC-CKF, the shape parameter and kernel size are respectively set as: $\sigma = 3$ and $\beta = 0.5$.
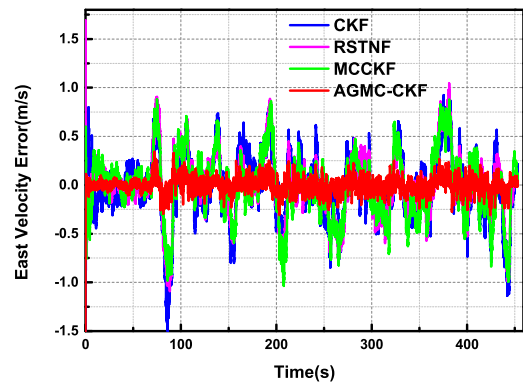
The velocity error and position error from the existing methods and the proposed method are respectively shown
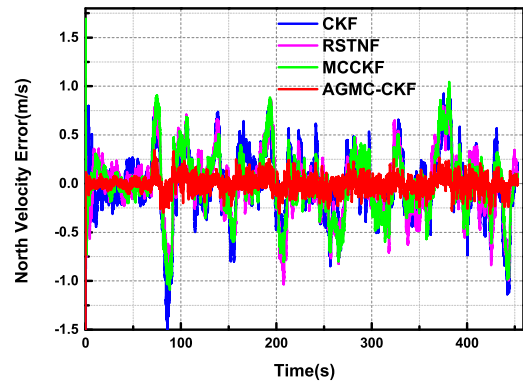
(a) North velocity error
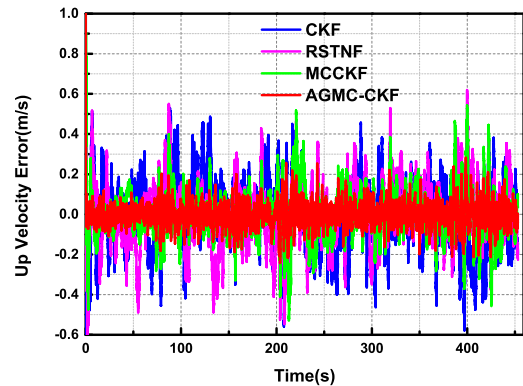
(b) Up velocity error

(c) East velocity error

FIGURE 12. Estimated Velocity errors of different filters.

in Figure. 12–Figure. 13, and the corresponding RMSE are listed in Table 2. It can be seen clearly that the RSTNF, MCCKF and the proposed AGMC-CKF all outperform the traditional CKF, owing to using the different robust technologies, i.e. the student's t-based variational Bayesian technology, the strong tracking based maximum correntropy technology and the proposed adaptive generalized maximum correntropy technology. The MCCKF performs better than the RSTNF, which demonstrates that the strong tracking based maximum correntropy technology more effective than the student's t-based variational Bayesian technology when simultaneously dealing with the process uncertainty and non-Gaussian measurement noise. We can also see that the proposed AGMC-CKF outperforms the MCCKF. This
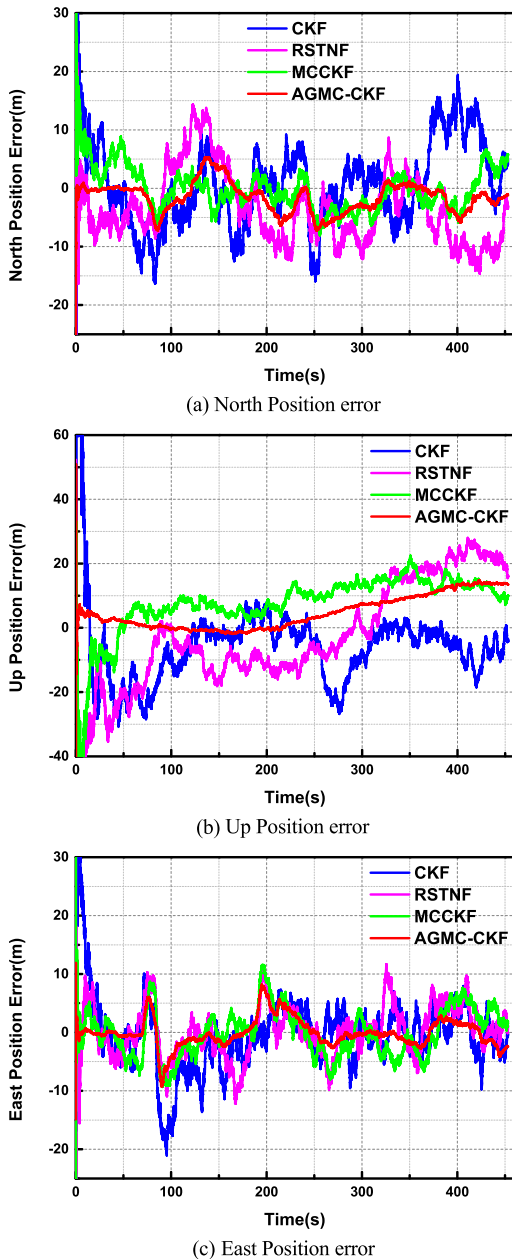
(a) North Position error

(b) Up Position error

(c) East Position error

FIGURE 13. Estimated Position errors of different filters.

TABLE 2. RMSEs of velocity and position from different algorithms.

Filters	RMSE					
	PosN (m)	PosU (m)	PosE (m)	VelN (m/s)	VelU (m/s)	VelE (m/s)
CKF	7.74	17.47	6.95	0.39	0.18	0.34
RSTNF	7.08	25.99	4.55	0.38	0.16	0.33
MCCKF	4.12	12.27	4.16	0.35	0.13	0.32
Proposed	3.80	8.06	2.42	0.07	0.05	0.06

V. CONCLUSION

In this paper, we focused on the handling of the process uncertainty and non-Gaussian measurement noise of the SINS/GNSS integrated navigation system induced by the vehicle's severe maneuver and abnormal measurement of GNSS. A new robust cubature Kalman filter based on the adaptive generalized maximum correntropy approach (termed AGMC-CKF) is proposed. The proposed new robust CKF suppresses the uncertain process noise via the adaptive forgetting recursive least square method and provides robustness against non-Gaussian measurement noise via the generalized maximum correntropy approach, based on which a new criterion termed adaptive generalized maximum correntropy (AGMC) criterion for SINS/GNSS integration is constructed. A new robust cubature Kalman filter for SINS/GNSS integration is derived utilizing the constructed AGMC criterion, where the predicted state vector and received measurements are processed simultaneously based on the regression form derived via the statistical linearization approach, and the parameters of the AGMC are updated adaptively via the adaptive forgetting scheme. Car-mounted experiments carried out on the SINS/GNSS integrated navigation system demonstrate the effectiveness and robustness of the proposed method.

APPENDIX
A. THE DEFINATION OF MAXIMUM CORRENTROPY
Correntropy is defined as a local and nonlinear similarity measure between two random variables. Given two scalar random variables X and Y, their correntropy is presented mathematically as [32], [33]:

$$V(X, Y) = E[\kappa(X, Y)] = \int \kappa(X, Y) \, dF_{XY}(X, Y) \quad (50)$$

where $E[\cdot]$ is the expectation operator, $k(.,.)$ represents the shift-invariant Mercer's type positive definite kernel function, $F_{XY}(X, Y)$ denotes the joint probability density function of X and Y. Given a finite number of samples $\{X_i, Y_i\}_{i=1}^{N}$ drawn from the joint probability density function $F_{XY}(X, Y)$, the correntropy can be estimated by using the sample estimator with N data points as follow:

$$\hat{V}(X, Y) = \frac{1}{N} \sum_{i=1}^{N} \kappa(X_i, Y_i) \quad (51)$$

is not surprising since the GMCC in general works better than the MCC under the condition of non-Gaussian. On the other hand, it has been proven that our proposed adaptive fading factor determination method is superior to the strong tracking filter technology. However, the better performance is achieved at the price of slightly higher computational costs. Therefore, we can conclude that our proposed robust framework is able to deal with the process uncertainty and non-Gaussian measurement noise effectively and can achieve better performance than the existing robust filters under the condition of the vehicle's severe maneuver and abnormal measurements in SINS/GNSS integrated navigation system.

In general, the kernel function is chosen as the Gaussian kernel:

$$\kappa\left(X, Y\right) = G_\sigma\left(X - Y\right) = \exp\left(-\frac{\|X - Y\|^2}{2\sigma^2}\right) \quad (52)$$

where $\sigma > 0$ is the kernel bandwidth, $G_\sigma\left(\cdot\right)$ is the Gaussian kernel function.

Compared with the mean square error (MSE) which uses the second-order statistic information (mean and variance) of the error, the correntropy contains a weighted sum of all even order moments of the error between the desired signal and filter output, making it being more sensitive to the heavy-tailed non-Gaussian noise. Thus, given a sequence of the data $\{X_i, Y_i\}_{i=1}^N$, the optimal solution can be obtained by maximum the correntropy as follows:

$$\hat{\mathbf{X}} = \arg\max_X \frac{1}{N} \sum_{i=1}^N \kappa\left(X_i, Y_i\right) \quad (53)$$

REFERENCES

[1] P. D. Groves, *Principles of GNSS, Inertial, and Multisensor Integrated Navigation Systems*. Norwood, MA, USA: Artech House, 2013.

[2] J. Farrell, *Aided Navigation: GPS With High Rate Sensors*. New York, NY, USA: McGraw-Hill, 2008.

[3] J. Farrell and M. Barth, *The Global Positioning System and Inertial Navigation*, vol. 61. New York, NY, USA: McGraw-Hill, 1999.

[4] B. Cui, X. Chen, Y. Xu, H. Huang, and X. Liu, "Performance analysis of improved iterated cubature Kalman filter and its application to GNSS/INS," *ISA Trans.*, vol. 66, pp. 460–468, Jan. 2017.

[5] K. Feng, J. Li, X. Zhang, X. Zhang, C. Shen, H. Cao, Y. Yang, and J. Liu, "An improved strong tracking cubature Kalman filter for GPS/INS integrated navigation systems," *Sensors*, vol. 18, no. 6, p. 1919, Jun. 2018.

[6] D. Simon, *Optimal State Estimation: Kalman, H Infinity, and Nonlinear Approaches*. Hoboken, NJ, USA: Wiley, 2006.

[7] M. Liu, J. Lai, Z. Li, and J. Liu, "An adaptive cubature Kalman filter algorithm for inertial and land-based navigation system," *Aerosp. Sci. Technol.*, vol. 51, pp. 52–60, Apr. 2016.

[8] Y. Huang and Y. Zhang, "A new process uncertainty robust Student's t based Kalman filter for SINS/GPS integration," *IEEE Access*, vol. 5, pp. 14391–14404, 2017.

[9] M. Zhong, J. Guo, and Q. Cao, "On designing PMI Kalman filter for INS/GPS integrated systems with unknown sensor errors," *IEEE Sensors J.*, vol. 15, no. 1, pp. 535–544, Jan. 2015.

[10] C. Hide, T. Moore, and M. Smith, "Adaptive Kalman filtering for low-cost INS/GPS," *J. Navigat.*, vol. 56, no. 1, pp. 143–152, Jan. 2003.

[11] I. Bilik and J. Tabrikian, "MMSE-based filtering in presence of non-Gaussian system and measurement noise," *IEEE Trans. Aerosp. Electron. Syst.*, vol. 46, no. 3, pp. 1153–1170, Jul. 2010.

[12] M. Karasalo and X. Hu, "An optimization approach to adaptive Kalman filtering," *Automatica*, vol. 47, no. 8, pp. 1785–1793, Aug. 2011.

[13] R. Mehra, "Approaches to adaptive filtering," *IEEE Trans. Autom. Control*, vol. AC-17, no. 5, pp. 693–698, Oct. 1972.

[14] D. H. Zhou and P. M. Frank, "Strong tracking filtering of nonlinear time-varying stochastic systems with coloured noise: Application to parameter estimation and empirical robustness analysis," *Int. J. Control*, vol. 65, no. 2, pp. 295–307, Sep. 1996.

[15] G. Hu, S. Gao, Y. Zhong, B. Gao, and A. Subic, "Modified strong tracking unscented Kalman filter for nonlinear state estimation with process model uncertainty," *Int. J. Adapt. Control Signal Process.*, vol. 29, no. 12, pp. 1561–1577, Dec. 2015.

[16] W. Huang, H. Xie, C. Shen, and J. Li, "A robust strong tracking cubature Kalman filter for spacecraft attitude estimation with quaternion constraint," *Acta Astronautica*, vol. 121, pp. 153–163, Apr. 2016.

[17] M. S. Arulampalam, S. Maskell, N. Gordon, and T. Clapp, "A tutorial on particle filters for online nonlinear/non-Gaussian Bayesian tracking," *IEEE Trans. Signal Process.*, vol. 50, no. 2, pp. 174–188, 2002.

[18] Z. Zhu, Z. Meng, Z. Zhang, J. Chen, and Y. Dai, "Robust particle filter for state estimation using measurements with different types of gross errors," *ISA Trans.*, vol. 69, pp. 281–295, Jul. 2017.

[19] J. Lim, "Particle filtering for nonlinear dynamic state systems with unknown noise statistics," *Nonlinear Dyn.*, vol. 78, no. 2, pp. 1369–1388, Oct. 2014.

[20] Y. Huang and Y. Zhang, "Robust student's t-based stochastic cubature filter for nonlinear systems with heavy-tailed process and measurement noises," *IEEE Access*, vol. 5, pp. 7964–7974, 2017.

[21] Y. Huang, Y. Zhang, N. Li, and J. Chambers, "Robust student'st based nonlinear filter and smoother," *IEEE Trans. Aerosp. Electron. Syst.*, vol. 52, no. 5, pp. 2586–2596, Oct. 2016.

[22] Y. Huang, Y. Zhang, B. Xu, Z. Wu, and J. Chambers, "A new outlier-robust student's t based Gaussian approximate filter for cooperative localization," *IEEE/ASME Trans. Mechatronics*, vol. 22, no. 5, pp. 2380–2386, Oct. 2017.

[23] X. Liu, H. Qu, J. Zhao, and P. Yue, "Maximum correntropy square-root cubature Kalman filter with application to SINS/GPS integrated systems," *ISA Trans.*, vol. 80, pp. 195–202, Sep. 2018.

[24] F. Wang, Y. He, S. Wang, and B. Chen, "Maximum total correntropy adaptive filtering against heavy-tailed noises," *Signal Process.*, vol. 141, pp. 84–95, Dec. 2017.

[25] B. Chen, X. Liu, H. Zhao, and J. C. Principe, "Maximum correntropy Kalman filter," *Automatica*, vol. 76, pp. 70–77, Feb. 2017.

[26] G. Y. Kulikov and M. V. Kulikova, "Estimation of maneuvering target in the presence of non-Gaussian noise: A coordinated turn case study," *Signal Process.*, vol. 145, pp. 241–257, Apr. 2018.

[27] Y. Huang, Y. Zhang, N. Li, Z. Wu, and J. A. Chambers, "A novel robust student'st-based Kalman filter," *IEEE Trans. Aerosp. Electron. Syst.*, vol. 53, no. 3, pp. 1545–1554, Jun. 2017.

[28] I. Arasaratnam and S. Haykin, "Cubature Kalman filters," *IEEE Trans. Autom. Control*, vol. 54, no. 6, pp. 1254–1269, Jun. 2009.

[29] J. H. Yoon, D. Y. Kim, and V. Shin, "Window length selection in linear receding horizon filtering," in *Proc. Int. Conf. Control, Automat. Syst.*, 2008, pp. 2463–2467.

[30] P. J. Huber, *Robust Statistics* (International Encyclopedia of Statistical Science). 1981, pp. 1248–1251.

[31] Z. Deng, L. Yin, B. Huo, and Y. Xia, "Adaptive robust unscented Kalman filter via fading factor and maximum correntropy criterion," *Sensors*, vol. 18, no. 8, p. 2406, Jul. 2018.

[32] G. T. Cinar and J. C. Príncipe, "Hidden state estimation using the correntropy filter with fixed point update and adaptive kernel size," in *Proc. Int. Joint Conf. Neural Netw. (IJCNN)*, 2012, pp. 1–6.

[33] H. Tang, *Information Theoretic Learning: Reny's Entropy and Kernel Perspectives*, J. Principe, Ed. IEEE Computational Intelligence Magazine, 2011.

KAIQIANG FENG received the B.S. and Ph.D. degrees from the Department of Instrument and Electronics, North University of China, Taiyuan, China, in 2015 and 2019, respectively. He is currently holding a postdoctoral position in armament science and technology. His current research interests include inertial navigation, inertial-based integrated navigation systems, and state estimation theory.

JIE LI was born in Lvliang, Shanxi, China, in 1976. He received the Ph.D. degree from the Department of Automation, Beijing University of Technology, Beijing, China, in 2005. He is currently a Professor of navigation, guidance and control with the North University of China, China. His current research interests include inertial sensing and control, inertial-based integrated navigation theory, and microsystem integration.

DEBIAO ZHANG was born in Jiaxiang, Shandong, China, in June 1989. He is currently pursuing the Ph.D. degree in instrument science and technology with the School of Instrument and Electronics, North University of China. He is also involved in research on inertial navigation.

JIANPING YIN was born in Yuxian, Shanxi, China, in 1975. He received the Ph.D. degree from the College of Mechatronics Engineering, North University of China, China, in 2010. He is currently a Professor of armament science and technology with the North University of China. His current research interests include munition damage technology and munition guidance technology.

● ● ●

XIAOKAI WEI was born in China, in 1992. He received the B.E. degree in weapon system and launch engineering from the College of Mechatronics Engineering, North University of China, Taiyuan, China, in 2015, where he is currently pursuing the Ph.D. degree in instrument science and technology. His current research interests include inertial navigation, integrated navigation, and adaptive control.